

The orbital evolution of the tidally stripped star and disk-driven stable mass transfer for QPEs in GSN 069

Di Wang

Department of Physics, Huazhong University of Science and Technology, Wuhan 430074, China

May 28, 2024

ABSTRACT

Context. The origin of the quasi-periodic eruptions (QPEs) is possibly mass loss at the periastron of a body moving around the supermassive black hole (SMBH) in a high eccentric orbit. Such a tidally stripped star is expected to radiate gravitational wave thereby leading to shrinkage of the periastron distance, and thus will eventually be disrupted by the SMBH in the previous studies.

Aims. This scenario predicts a gradually increasing mass transfer, contradicting the long term evolution of the observed intensity of the QPEs in GSN 069.

Methods. In this paper, we first revisited the orbital evolution of the stripped star. Then we suggested a model of a tidal stripped WD moving inside an accretion disk for QPEs in GSN 069.

Results. We found the effect of the mass transfer finally dominates the orbital evolution, resulting in the stripped star finally escaping the SMBH rather than being disrupted by it. The drag force by the disk can effectively reduce mass transfer and thus explain the observed long term evolution in the intensity of the QPEs in GSN 069. The disk is likely a fallback disk of the tidal disruption event in GSN 069. Considering the evolution of its accretion rate, the increase in the intensity of the latest eruption can also be explained.

1. Introduction

A white dwarf (WD) orbiting around a supermassive black hole (SMBH) with high eccentricity may lose mass each time through the periastron. Such a tidally stripped WD is not only expected to emit periodic electromagnetic wave signals (Zalamea et al. 2010), but also the target of space-based gravitational wave detectors such as Laser Interferometer Space Antenna (LISA) (Babak et al. 2017) and TianQin (Luo et al. 2016). The first discovered quasi-periodic eruptions (QPEs) from GSN 069 are suggested to possibly originate from a tidally stripped WD in a high eccentric orbit (Miniutti et al. 2019; Wang et al. 2022; King 2020).

Due to gravitational wave radiation decreasing the periastron distance, the mass loss of the tidally stripped WD gradually increases until finally the WD is tidally disrupted by the SMBH (Zalamea et al. 2010; Wang et al. 2022). However, the intensity of QPEs in GSN 069 shows no sign of increasing (Miniutti et al. 2023b,a), which is inconsistent with the previous prediction. King (2022) points out that the mass transfer stability requires the angular momentum transfer from the disk to the orbiting star, he suggested that orbital resonance with the disk possibly could accomplish this, but further discussion was lacking.

GSN 069 also has a tidal disruption event (TDE) that has lasted more than a decade (Shu et al. 2018; Sheng et al. 2021). This TDE was recently found to have re-brightened, and while it was brightening, the QPEs disappeared (Miniutti et al. 2023b). When radiation from the TDE faded again, the QPEs reappeared and were stronger than in the last outburst before they disappeared (Miniutti et al. 2023a). Such behavior implies that the evolution of mass transfer may be related to the accretion rate of the accretion disk.

The origin of this TDE is likely the disruption of a common envelope of the binary containing the current orbiting body before it is captured by the SMBH (Wang 2023). This means that the fallback disk of the TDE is nearly coplanar with the orbit of

the orbiting body that produced the QPEs. In this situation, the drag force by the disk may significantly affect the secular orbital evolution of the orbiting body.

In this paper, we first revisited the secular evolution of the tidally stripped star with high eccentricity taking into account the effect of the mass transfer on the orbit, which is ignored in the previous studies. We found that the effect of mass transfer significantly changes the criterion for unstable mass transfer. The mass transfer for WDs is no longer dynamically stable, while it remains dynamically stable for main sequence stars. Furthermore, the effect of the mass transfer dominates the secular orbital evolution, which leads to the fate of the stripped star escaping the SMBH rather than being disrupted by it.

While the origin of QPEs is still debated, there are various other models (Chen et al. 2022; Zhao et al. 2022; Wang et al. 2022; Krolik & Linial 2022; Lu & Quataert 2023; Xian et al. 2021; Suková et al. 2021; Linial & Sari 2023; Linial & Metzger 2023; Franchini et al. 2023). In this paper, we focus on the stripped WD model in a high eccentric orbit for GSN 069 (King 2020, 2022). We calculated the secular effect of drag force by the disk on the orbit for GSN 069. We found that the drag force can transfer the angular momentum of the disc to the stripped WD, and then stabilize the mass transfer. This effect is strongly dependent on the accretion rate, which can be estimated from the luminosity of the TDE. The derived change in mass transfer rate by the disk drag has the ability to suppress other effects that increase mass transfer, thus explaining the long-term evolution of the observed intensity of QPEs. The increase in the intensity of the QPEs after the TDE re-brightened can also be explained by this model.

This paper is organized as follows. In Section 2, we revisited the secular orbital evolution of the stripped star under the effect of gravitational wave radiation and mass transfer. In Section 3, we discuss the effect of drag force by the accretion disk on the orbit for QPEs in GSN 069. We made discussions in section 4 and a summary in Section 5.

2. Evolution with mass transfer and gravitational radiation

We consider a WD of mass M and radius R in a highly eccentric orbit around a SMBH of mass M_h . When it reaches the periastron, the stripped mass can be obtained by calculating the mass of the matter in the WD outside Roche lobe (Chen et al. 2023)

$$\frac{\Delta M}{M} \simeq 4.8 \left[1 - (M/M_{\text{ch}})^{4/3} \right]^{3/4} \left(1 - \frac{\beta_0}{\beta} \right)^{5/2}. \quad (1)$$

Here $\beta \equiv r_t/r_p$ is impact factor, where $r_t = R(M_h/M)^{1/3}$ is the disrupted radius and r_p is the periastron radius. The Chandrasekhar mass M_{ch} is $1.44M_\odot$ and β_0 is about 0.5. Mass transfer occurs only if β is greater than β_0 . And the WD is disrupted when β is greater than 1.

Differentiating it gives

$$\frac{\dot{\Delta M}}{\Delta M} = \frac{1 - 2(M/M_{\text{ch}})^{4/3}}{1 - (M/M_{\text{ch}})^{4/3}} \frac{\dot{M}}{M} + \frac{5\beta_0}{2(\beta - \beta_0)} \frac{\dot{\beta}}{\beta}. \quad (2)$$

The latter term is usually dominant because β is close to β_0 when mass transfer is not extremely high. Setting the mass-radius index ζ which gives mass-radius relation $R \propto M^\zeta$, the $\dot{\beta}$ can be obtained by (King 2022)

$$\frac{\dot{\beta}}{\beta} = \frac{2\dot{M}}{M} \left(\frac{5}{6} + \frac{\zeta}{2} - q \right) - \frac{2\dot{J}}{J} + \frac{\dot{e}}{1+e}. \quad (3)$$

Here $q = M/M_h$ is the mass ratio, J is the total orbital angular momentum and e is the orbital eccentricity.

2.1. Mass transfer

The mass-radius relation of the WD is (Paczynski 1971)

$$R = 9 \times 10^8 \left[1 - \left(\frac{M}{M_{\text{ch}}} \right)^{4/3} \right]^{1/2} \left(\frac{M}{M_\odot} \right)^{-1/3} \text{ cm}, \quad (4)$$

which is adopted in the derivation of Eq. (1) (Chen et al. 2023). So ζ for the WD is about -1/3 for low mass, and more negative when mass is close to M_{ch} . And it is always greater than -5/3 so that the first term in Eq. (3) is negative, which can suppress mass transfer. King (2022) claim that this term is dominant on short timescales so that the mass transfer is dynamically stable. However, he ignored the \dot{e} caused by the mass transfer, which is¹ (Sepinsky et al. 2007b)

$$\langle \dot{e} \rangle_{\dot{M}} = -2(1+e) \frac{\dot{M}}{M} (1-q). \quad (5)$$

Substituting it into Eq. (3) gives

$$\left\langle \frac{\dot{\beta}}{\beta} \right\rangle_{\dot{M}} = \frac{\dot{M}}{M} \left(\zeta - \frac{1}{3} \right). \quad (6)$$

Here $\langle \dot{J}/J \rangle \approx 0$, because only very little angular momentum is removed by central SMBH via accretion (King 2022).

So the self-driven mass transfer for the WDs is unstable. Noted that Eq. (5) show that orbit is more eccentric under mass

¹ Wang et al. (2022) had considered the effect of the mass transfer on the orbit too. Their formula is different from this because they mistake the instantaneous mass transfer rate in Sepinsky et al. (2007b) for the secular mass transfer rate thus underestimate this effect.

transfer, and the change of the semi-major axis (Sepinsky et al. 2007b),

$$\left\langle \frac{\dot{a}}{a} \right\rangle_{\dot{M}} = -2 \frac{1+e}{1-e} \frac{\dot{M}}{M} (1-q), \quad (7)$$

is positive. So unstable mass transfer would lead to the eventual escape of the WD, contrary to the prediction that gravitational radiation would lead to the disruption of the WD (Zalamea et al. 2010; Wang et al. 2022).

2.2. Gravitational radiation

The change of orbit caused by the gravitational radiation is (Peters 1964)

$$\left\langle \frac{\dot{J}}{J} \right\rangle_{\text{GW}} = -\frac{32}{5} \frac{G^3 M M_h M_t}{c^5 a^4 (1-e^2)^{5/2}} \left(1 + \frac{7}{8} e^2 \right), \quad (8)$$

$$\left\langle \frac{\dot{a}}{a} \right\rangle_{\text{GW}} = -\frac{64}{5} \frac{G^3 M M_h M_t}{c^5 a^4 (1-e^2)^{7/2}} \left(1 + \frac{73}{24} e^2 + \frac{37}{96} e^4 \right), \quad (9)$$

$$\langle \dot{e} \rangle_{\text{GW}} = -\frac{304}{15} e \frac{G^3 M M_h M_t}{c^5 a^4 (1-e^2)^{5/2}} \left(1 + \frac{121}{304} e^2 \right). \quad (10)$$

Here G is the gravitational constant, $M_t = M_h + M$ is total mass and c is the speed of light. Substituting Eq. (8) and (10) into Eq. (3) yields

$$\left\langle \frac{\dot{\beta}}{\beta} \right\rangle_{\text{GW}} = \frac{64}{5(1+e)} \frac{G^3 M M_h M_t}{c^5 a^4 (1-e^2)^{5/2}} \left(1 - \frac{7}{12} e + \frac{7}{8} e^2 + \frac{47}{192} e^3 \right), \quad (11)$$

which is positive. So both mass transfer and gravitational radiation enhance mass transfer, but gravitational wave radiation reduces a and e , which is the opposite of the effect of mass transfer.

2.3. Orbital Evolution for the WD

The effect of the gravitational radiation is stronger than the effect of the mass transfer when the mass transfer rate is low. As the mass transfer rate gets higher, the effect of mass transfer becomes dominant. While factor $1/(1-e)$ evolves to very high values, the effect of gravitational radiation becomes smaller. Because the periastron $r_p = a(1-e)$ is constant under mass transfer, $\langle \dot{r}_p \rangle_{\dot{M}} = 0$, which make the effect of gravitational radiation proportional to $(1-e)^{1/2}$ for \dot{a}/a and $(1-e)^{3/2}$ for \dot{J}/J and \dot{e} when $e \approx 1$.

The mass transfer rate $|\dot{M}|$ doesn't grow endlessly. Because \dot{M} is related not only to ΔM but also to the orbital period P_b , $\dot{M} = -\Delta M/P_b$. And the a grows dramatically at high e , as does the P_b . When the growth rate of P_b is greater than the growth rate of ΔM , $|\dot{M}|$ will start to decrease until the WD escapes. And the critical condition can be obtained by

$$\frac{\dot{M}}{M} = \frac{\dot{\Delta M}}{\Delta M} - \frac{3}{2} \frac{\dot{a}}{a} \approx \left[\frac{5\beta_0}{2(\beta - \beta_0)} \left(\zeta - \frac{1}{3} \right) + 3 \frac{1+e}{1-e} \right] \frac{\dot{M}}{M} = 0. \quad (12)$$

So the WD finally escapes with eccentricity $e_f \gtrsim 1$, then the total mass it loses can be obtained from Eq. (5)

$$-\frac{\Delta M}{M} \approx \frac{e_f - e_i}{2(1+e_i)(1+q)} \approx \frac{1-e_i}{4(1+e_i)}, \quad (13)$$

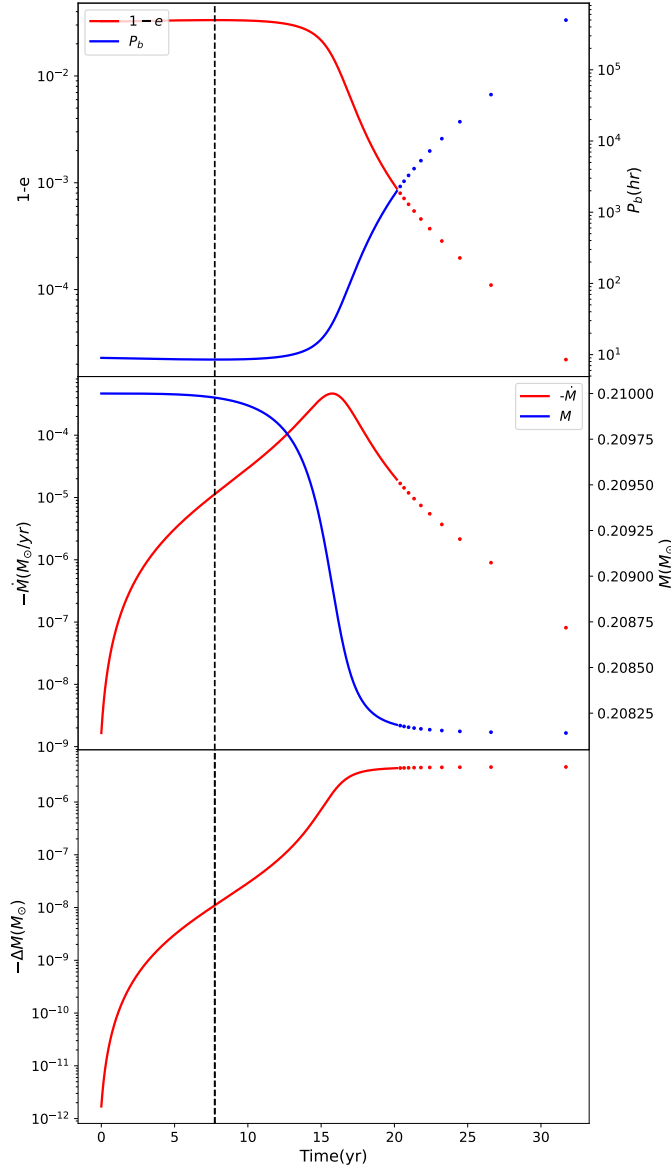


Fig. 1. The evolution of orbit parameters and WD's mass. The first panel from top to bottom shows the evolution of $1 - e$ and orbital period P_b . The second one is the evolution of the average mass transfer rate and mass of the WD. And the last one represents the evolution of mass loss at periastron. The dashed line represents the critical time that the effect of the mass transfer becomes dominant. For each parameter, the critical times are not the same but very close. Here we use the critical time of e for all panels. The last 10 orbits are plotted as scatter plots and the rest as line plots.

where $q \ll 1$ and e_i is the initial eccentricity while the effect of the mass transfer is dominant. The WD loses at most 1/4 of its total mass and can survive the mass loss.

Here we show an example of the evolution under mass transfer and gravitational radiation in Fig. 1. We adopt possible parameters of GSN 069: $P_b = 9$ hr, $M_h = 5 \times 10^5 M_\odot$ and $M = 0.21 M_\odot$. Then $e = 0.968$ can be obtained from Eq. (4) with $\beta \approx \beta_0$. The initial β is 0.50001. The orbital parameters and the mass and radius of the WD are updated each time the WD passes through the periastron. We use $\langle \dot{r}_p \rangle$ and $\langle \dot{e} \rangle$ to evolve orbit, because $\langle \dot{a}/a \rangle$ is too high to properly represent orbital changes in the above method when $1 - e$ is very small. Evolution will stop when e is greater than 1.

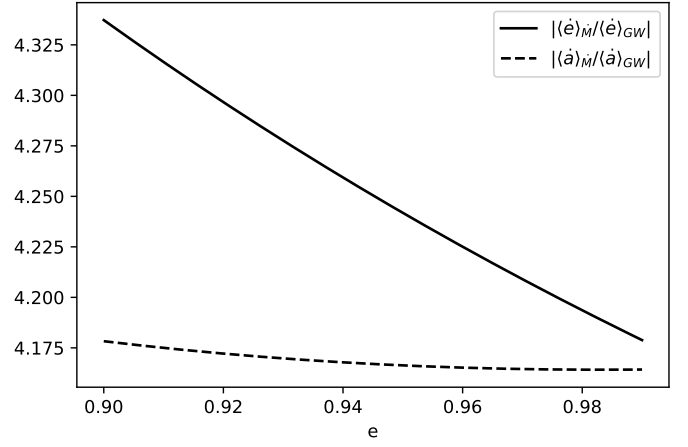


Fig. 2. Comparison of $\langle \dot{a} \rangle$ and $\langle \dot{e} \rangle$ caused by the mass transfer and gravitational radiation with $\langle \beta \rangle = 0$. Here η is taken as 2/3.

As shown in Fig. 1, the mass loss is rapidly enhanced after the effects of mass transfer dominate. When the resulting increase in orbital period exceeds the increase in mass loss, ΔM becomes stable. During this process, the eccentricity keeps growing rapidly until it exceeds 1 and the WD escapes from the SMBH. The period of the last few orbits can vary significantly.

2.4. Orbital Evolution for the main-sequence star

If ζ of the stripped star is greater than 1/3, such as a main-sequence star, then the mass transfer will stabilize itself, and $\langle \beta \rangle$ will evolve towards 0. Once this happens, $\langle \beta \rangle = 0$ will remain. Since the timescale of the mass transfer evolution is larger than that of the orbital parameter evolution, \dot{M} can be able to adjust itself rapidly to balance with the effects of gravitational radiation in the secular evolution. That is, it always satisfies

$$\left\langle \frac{\dot{\beta}}{\beta} \right\rangle = \left\langle \frac{\dot{\beta}}{\beta} \right\rangle_M + \left\langle \frac{\dot{\beta}}{\beta} \right\rangle_{GW} \approx 0. \quad (14)$$

While these two effects are balanced on $\langle \dot{\beta} \rangle$, they are not balanced on $\langle \dot{a} \rangle$ and $\langle \dot{e} \rangle$. As shown in Fig. 2, the effect of the mass transfer is always dominant when $\langle \beta \rangle = 0$, but it is of the same magnitude as GW. Thus, the evolution of a stripped main-sequence is similar to that of a WD, but on a much longer timescale, the gravitational radiation timescale, because \dot{M} is driven by gravitational radiation.

We show an example in Fig. 3. The initial orbital parameters are $M_h = 5 \times 10^5 M_\odot$, $M = 0.1 M_\odot$, $\beta = 0.50004$ and $P_b = 40$ hr. The radius is obtained by $R = 1.06(M/M_\odot)^{0.945} R_\odot$ (Demircan & Kahraman 1991). Then the eccentricity can be obtained $e = 0.912$.

As shown in Fig. 3, the effect of mass transfer is initially weak and $|\dot{M}|$ increase rapidly driven by gravitational radiation, and then reaching balance $\langle \beta \rangle = 0$. At this point, the evolution of the orbit is dominated by the effects of mass transfer, with r_p remaining almost constant while e grows. Since $\langle \dot{\beta}/\beta \rangle_{GW}$ scales as $(1 - e)^{3/2}$, $|\dot{M}|$ coupled to it will keep decreasing. Eventually, like WDs, main sequence stars escape from SMBH, but on much longer timescales.

There is also a special case where, if the initial $|\dot{M}|$ and e are both high, e may evolve to greater than 1 before the $|\dot{M}|$ has had time to be reduced to balance state. In addition, in the final stages of evolution, when the orbital period is growing rapidly, there is

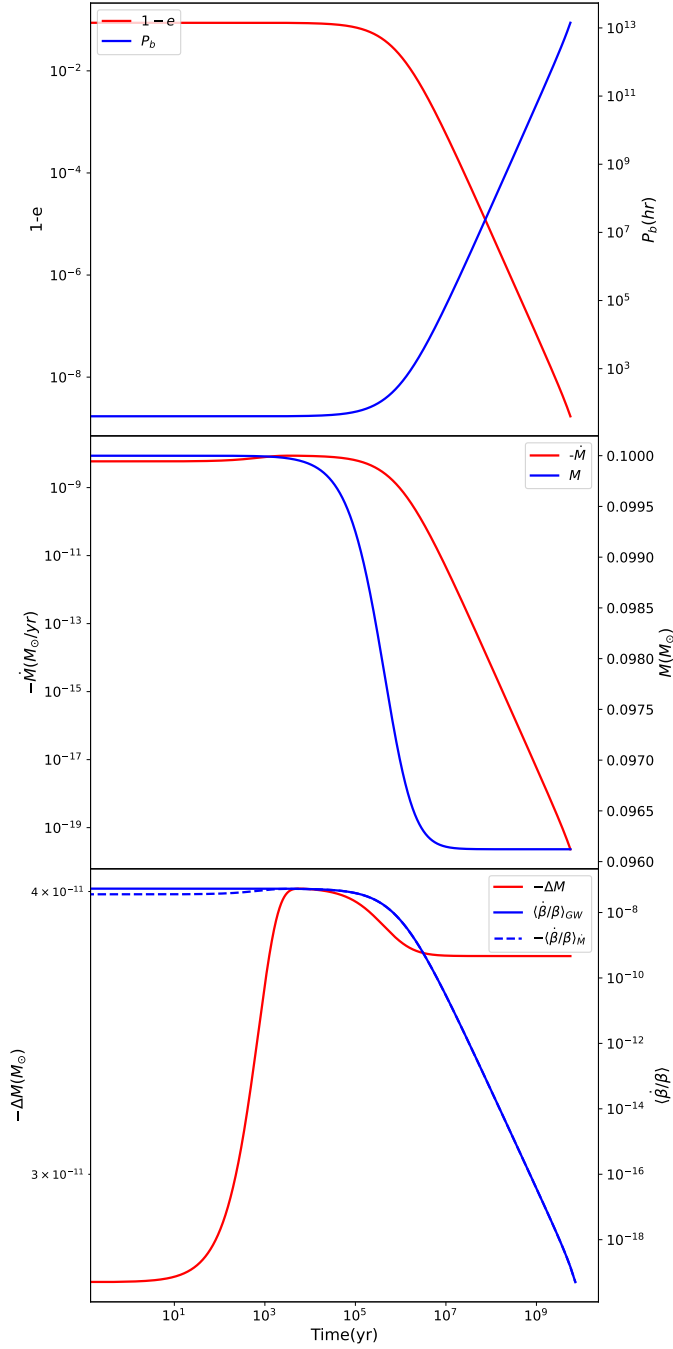


Fig. 3. Similar as Fig. 1, but for main-sequence star. The last panel from the top also shows the evolution of $\langle\beta\rangle$ of gravitational radiation and mass transfer.

a possibility that the star may be perturbed by other gravitational sources away from the black hole and thus escape early.

2.5. Comparison with the observation of QPEs

Before QPEs from GSN 069 disappeared, its peak intensity in 0.4–1 keV decays dramatically (Miniutti et al. 2023b). However, the bolometric luminosity by assuming absorbed black-body spectrum was almost constant for each observation, except for the last one, where it was reduced by roughly half (Miniutti et al. 2023a). If the bolometric luminosity is positively corre-

lated with the mass loss of the star at the periastron, such result implies that β is constant and then gets smaller.

Assuming the QPEs is caused by the mass transfer via Roche-lobe overflow, the orbiting star should be a WD for GSN 069 (King 2020). As shown in Fig. 1, the mass loss for WD grows rapidly except in the final stage of evolution, when the orbital period also grows rapidly. There was no significant change in the period of QPEs in GSN 069. So a mechanism for stabilizing mass transfer is required to explain the long-term evolution of QPEs, and the drag of a gaseous disk may achieve this.

3. Evolution driven by the accretion disk

3.1. Drag force by the accretion disk

The drag force caused by the accretion disk can be expressed as

$$\mathbf{a} = -\frac{\mathbf{v}_{rel}}{\tau_F}. \quad (15)$$

Here $\mathbf{v}_{rel} = \mathbf{v} - \mathbf{v}_k$ is the relative velocity of the star with respect to the local gas, where \mathbf{v} is the speed of star and the keplerian velocity \mathbf{v}_k is the velocity of the local gas. The timescale τ_F of the drag force, which is considered as hydrodynamic force or dynamical friction. The hydrodynamic timescale is (Szölgény et al. 2022)

$$\tau_H = \frac{2M}{C_D \pi R^2 \rho_g v_{rel}}. \quad (16)$$

Here C_D is related to the shape of the star, and equals 1 for a sphere, and ρ_g is the density of the local gas. The timescale of the dynamical friction is (Ostriker 1999)

$$\tau_D = \frac{v_{rel}^3}{4\pi G^2 M \rho_g F(\mathcal{M})}, \quad (17)$$

where $F(\mathcal{M})$ is

$$F(\mathcal{M}) = \begin{cases} \frac{1}{2} \ln \left(\frac{1+\mathcal{M}}{1-\mathcal{M}} \right) - \mathcal{M}, & 0 < \mathcal{M} < 1, \\ \frac{1}{2} \ln \left(1 - \frac{1}{\mathcal{M}^2} \right) + \ln \left(\frac{r}{R} \right), & \mathcal{M} > 1. \end{cases} \quad (18)$$

Here $\mathcal{M} = v_{rel}/c_s$ is the Mach number where c_s is the local sound speed. And r is the characteristic size, and we adopted the distance from the central black hole.

The change of the specific angular momentum $h = \sqrt{G(M_h + M)a(1-e)}$ caused by the drag force can be obtained by

$$\frac{\dot{h}}{h} = -\frac{1}{h\tau_F} \mathbf{r} \times \mathbf{v}_{rel} = \frac{1}{\tau_F} \left(\frac{\chi}{\sqrt{1+e\cos f}} - 1 \right), \quad (19)$$

where f is the true anomaly, and χ is 1 for the prograde star and -1 for the retrograde star. And the change of the specific energy $K = -G(M_h + M)/2a$ is

$$\frac{\dot{K}}{K} = -\frac{1}{K\tau_F} \mathbf{v} \cdot \mathbf{v}_{rel} = \frac{2}{\tau_F} \left(\frac{(1+2e\cos f + e^2) - \chi(1+e\cos f)^{3/2}}{1-e^2} \right). \quad (20)$$

The secular evolution can be obtained by averaging them over an orbital period. Then the secular evolution of orbital parameters are

$$\left\langle \frac{\dot{a}}{a} \right\rangle_{disk} = -\left\langle \frac{\dot{K}}{K} \right\rangle, \quad (21)$$

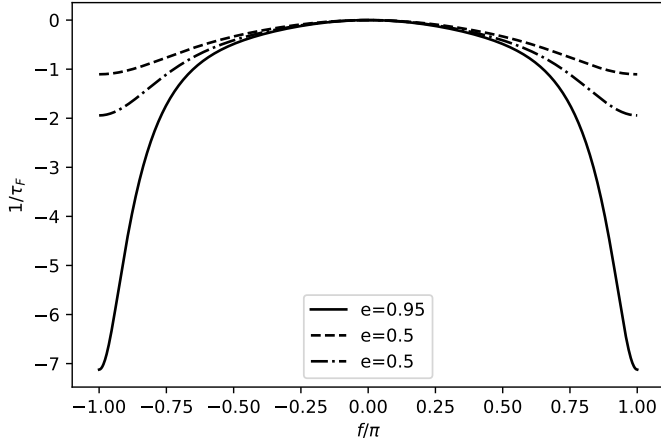


Fig. 4. $\dot{\beta}/\beta$ with true anomaly for different eccentricity. For all eccentricity, $\dot{\beta}/\beta$ is always negative and equal to zero while $f = 0$.

$$\langle \dot{e} \rangle_{\text{disk}} = -\frac{1-e^2}{e} \left(\left\langle \frac{\dot{h}}{h} \right\rangle + \frac{1}{2} \left\langle \frac{\dot{K}}{K} \right\rangle \right), \quad (22)$$

and the change of β is

$$\left\langle \frac{\dot{\beta}}{\beta} \right\rangle_{\text{disk}} = -\frac{1+e}{e} \left\langle \frac{\dot{h}}{h} \right\rangle - \frac{1-e}{2e} \left\langle \frac{\dot{K}}{K} \right\rangle. \quad (23)$$

While near the periastron, the velocity of the orbiting star is greater than the Keplerian velocity and is therefore slowed down, as it moves away from the periastron, its velocity becomes less than the Keplerian velocity and is therefore accelerated. Since the latter interaction time is longer, star will likely gain angular momentum from the accretion disk and thus reduce the β .

Eq. (23) can also be used to calculate instantaneous $\dot{\beta}/\beta$ for different f , as shown in Fig. 4. Even for a star near the periastron, β is still positive, so the drag force by the disk can always suppress mass transfer.

3.2. Application on GSN 069

3.2.1. Stable mass transfer

We consider an α standard disk with $\alpha = 0.1$ and $M_h = 5 \times 10^5 M_\odot$. The density and sound speed can be calculated for a given accretion rate \dot{M}_{Acc} in the unit of Eddington accretion rate \dot{M}_{Edd} (radiation efficiency $\eta = 0.1$). As shown in Fig. 5, the hydrodynamic force is always stronger than the dynamical friction in all orbital phases, thus dominant on the effect by disk. We only consider the hydrodynamic force in the following calculation.

The secular evolution of orbital parameters is shown in Fig. 6. For varies \dot{M}_{Acc} and e , a prograde WD always gains angular momentum and loses energy from the accretion disk, which decreases β , a and e . A retrograde WD shows different evolution, as shown in Fig. 7. The angular momentum is transferred from it to the accretion disk, which makes β increase. The energy is still transferred from the WD to the accretion disk. They make β increase and a still decrease. And e continues to decrease at low \dot{M}_{Acc} but increases at high \dot{M}_{Acc} .

The different dependence of the parameter evolution on \dot{M}_{Acc} at high and low \dot{M}_{Acc} is because the inner region of the accretion disk is dominated by radiation pressure at high \dot{M}_{Acc} and gas pressure at low \dot{M}_{Acc} . Therefore, the disk density decreases with

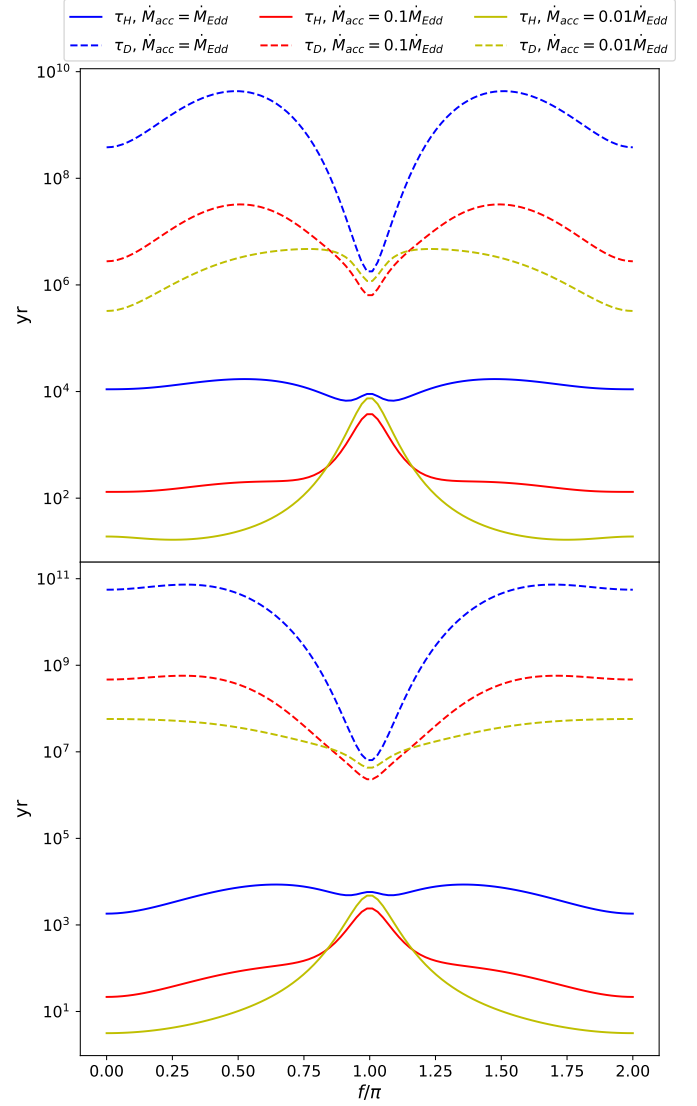


Fig. 5. Timescales with true anomaly for the hydrodynamic force and dynamical friction for a WD with $M = 0.21 M_\odot$, $P_b = 9$ hr and $e = 0.95$. The upper panel is for the prograde star and the lower panel is for the retrograde star. Solid lines and dashed lines represent the timescales of the hydrodynamic force and dynamical friction, respectively. Different colors represent the different accretion rate of the disk.

increasing \dot{M}_{Acc} for radiation pressure dominance resulting in a decrease in drag force, while the disk density increases with increasing \dot{M}_{Acc} for gas pressure dominance increasing drag force.

A prograde WD is preferred for GSN 069. The WD may be captured from a binary system by the Hill mechanism (Hills 1988; Wang et al. 2022). The accretion disk is likely to be a fallback disk from a TDE, which is possibly a disruption of the common envelope of the binary system (Wang 2023). In this scenario, the WD is prograde.

Here we adopt the results in Miniutti et al. (2023b). Assuming radiation efficiency $\eta = 0.1$, the accreted mass is about $3.7 \times 10^{-8} M_\odot$, corresponding to $\dot{M}/M \approx -1.7 \times 10^{-4} \text{ yr}^{-1}$ and $\beta \approx 0.5005$ with $M = 0.21 M_\odot$. The change of β induced by mass transfer is $\langle \dot{\beta}/\beta \rangle_M \approx 1.1 \times 10^{-4} \text{ yr}^{-1}$ with $\zeta = -1/3$. The bolometric luminosity of TDE is about 10^{44} erg/s corresponding to $\sim 1.6 \dot{M}_{\text{Edd}}$. Assuming $e = 0.95$, it predicts $\langle \dot{\beta}/\beta \rangle_{\text{disk}} \approx -3.5 \times 10^{-4} \text{ yr}^{-1}$ as shown in Fig. 6. The effects of disk drag and

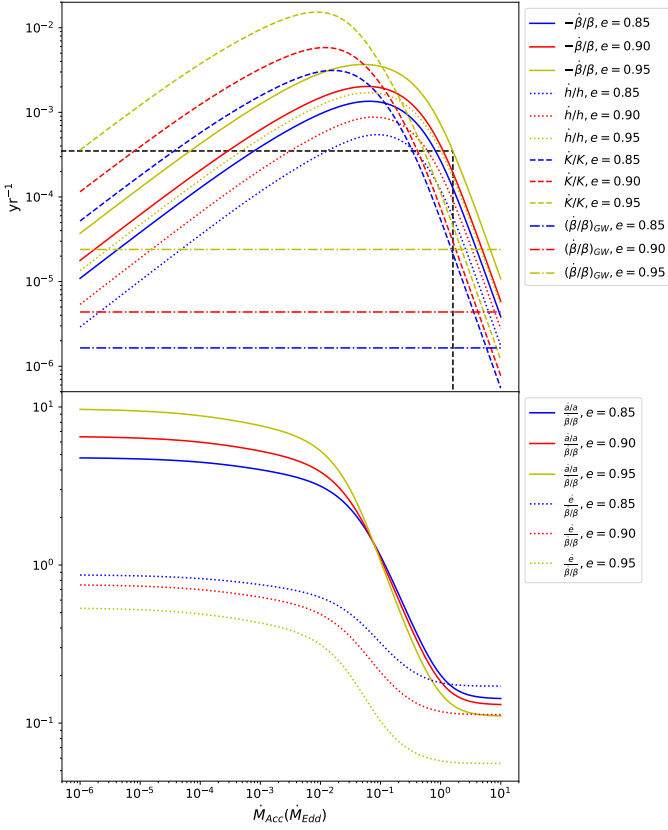


Fig. 6. Secular change of orbital parameters caused by hydrodynamic force for a prograde WD with $M = 0.21 M_{\odot}$ and $P_b = 9$ hr under different accretion rate. The top panel shows the change of β , specific angular momentum, and specific orbital energy caused by drag force, it also shows the effect on β caused by gravitational radiation for comparison. The dashed black line represents the point with \dot{M}_{Acc} of GSN 069 and $e = 0.95$, it predicts $\dot{\beta}/\beta \approx -3.5 \times 10^{-4} \text{ yr}^{-1}$ (see texts). The bottom panel represents the change of the a and e relative to β .

mass transfer on β are in the same order of magnitude, suggesting that disk drag has the ability to stabilize mass transfer.

3.2.2. History and future of evolution

Early in the TDE, there is a high accretion rate of the fallback disk, resulting in weak drag force by the disk. The evolution of β is dominant by the mass transfer or gravitational wave radiation. Thus, the intensity of QPEs kept increasing during this stage. QPEs can be observed when the intensity of QPEs is higher than TDE. It is consistent with the fact that QPEs in GSN 069 do not accompany the TDE at the same time, but appear suddenly during the decay of the TDE (Miniutti et al. 2023b).

As the accretion rate decreases, drag force by the disk begins to dominate $\dot{\beta}$, and at that point the intensity of the QPEs begins to decrease. When the TDE rebrighten, the increased accretion rate led to a weaker drag force and thus an increase in the mass transfer. Then, when the accretion rate begins to decrease again, the effect of the drag force enhances and the intensity of QPEs will keep decreasing. After switching from radiation pressure dominance to gas pressure dominance in the inner region of the disk, the drag force decreases with decreasing accretion rate. When β is dominated by gravitational wave radiation, the mass transfer begins to enhance. When β is dominated by mass

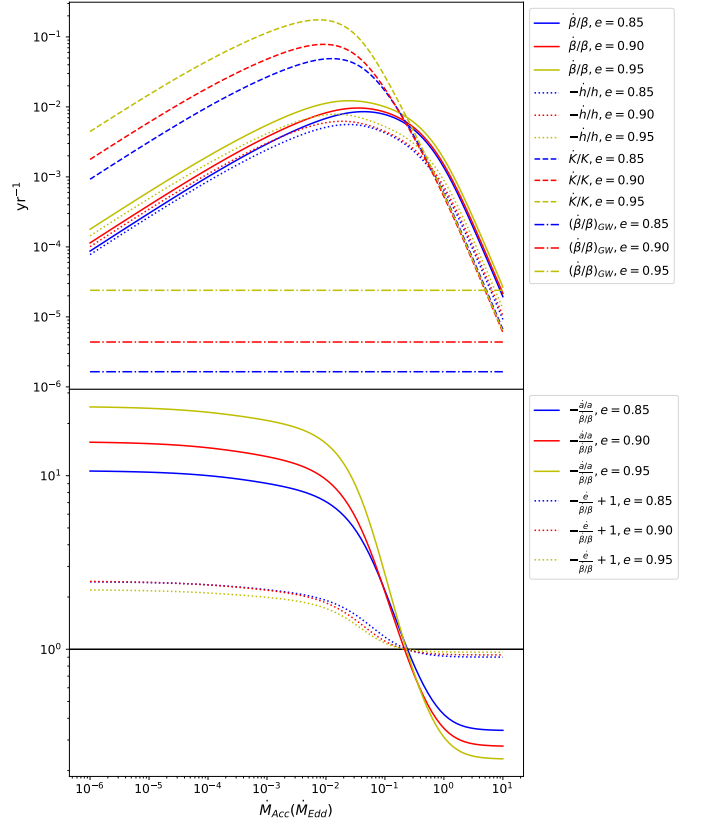


Fig. 7. As in Fig. 6, but for a retrograde WD. The sign of $\dot{\beta}/\beta$, \dot{h}/h , $(\dot{a}/a)/(\dot{\beta}/\beta)$, and $\dot{e}/(\dot{\beta}/\beta)$ is changed. To show value of $-\dot{e}/(\dot{\beta}/\beta)$ in the logarithmic axis, we add 1 on them, because they change sign at high \dot{M}_{Acc} .

transfer, the unstable mass transfer leads to WD escape from the SMBH.

While the accretion rate decreases, the outer radius of the fallback disk may change (Shen & Matzner 2014). The orbital semi-long axis of the stripped WD may be larger than the outer radius of the disk. In this situation, the drag force by the disk acts only on that side of the periastron. The secular evolution of the orbital parameters can be obtained by considering drag force only at $-\kappa\pi < f < \kappa\pi$ when averaging them over an orbit. Here κ ranges from 0 to 1. As shown in Fig. 8, the secular evolution of orbital parameters is significantly affected by κ , especially for $\dot{\beta}/\beta$. When $\kappa < 0.5$, the drag force only acts near the periastron, thus the angular momentum of the stripped WD is transferred to the disk as expected.

Even though the change in the outer radius of the disk affects the evolution of β , the tendency for the effect of the drag force by the disk to diminish is constant. Therefore, β will start to grow when the effect of gravitational wave radiation exceeds the drag force by the disk. Finally, the stripped WD will escape from SMBH after entering self-unstable mass transfer, as described by Section 2.

3.2.3. Secular evolution of GSN 069

Due to the evolution on the accretion rate of the fallback disk in GSN 069, the secular evolution on mass transfer may experience complex changes. Fig. 9 show an example with possible parameters of GSN 069. Following the formula in Miniutti et al. (2023b), the accretion rate of each peak for TDE is described by

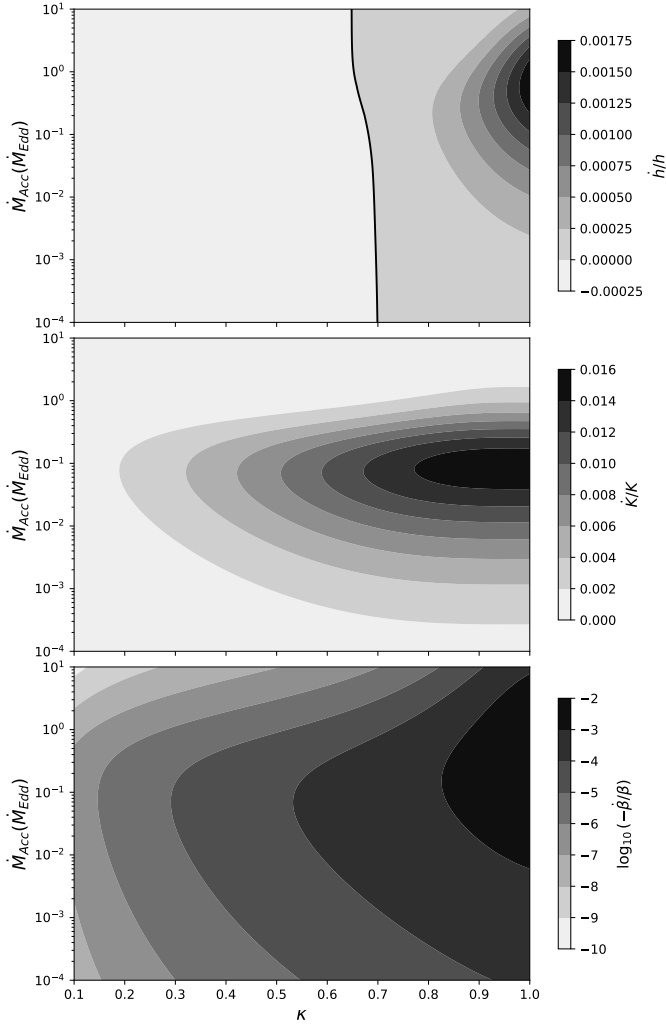


Fig. 8. Distribution of secular change of orbital parameters for different \dot{M}_{Acc} and κ . The top, middle and bottom panels represent h/h , K/K and $\dot{\beta}/\beta$, respectively. They are obtained with the drag force acting only when true anomaly f is within $-\kappa\pi$ to $\kappa\pi$. The solid line in the top panel represents the $h = 0$.

$$\dot{M} = \dot{M}_{\text{peak}} \times \begin{cases} e^{-(t-t_{\text{peak}})^2/2\sigma^2} & t \leq t_{\text{peak}} \\ \left[\frac{(t-t_{\text{peak}}+t_0)}{t_0} \right]^n & t > t_{\text{peak}} \end{cases}, \quad (24)$$

where the parameters can be obtained by fitting the light curve (Miniutti et al. 2023b). For the first peak, $t_0 = 7.6$ years and $t_{\text{peak}} = 600$ days, only the decay phase is calculated. For the second peak, $t_0 = 4.8$ year, $t_{\text{peak}} = 3850$ days and $\sigma = 400$ days. And n is $-9/4$ for each peak, \dot{M}_{peak} is $9 \dot{M}_{\text{Edd}}$ for the first peak and $6.3 \dot{M}_{\text{Edd}}$ for the second peak. The orbital parameters are same as them in Section 3.2.1, while the time is setting to 7 years. Then the past and future evolution can be obtained by the same method in Section 2.3.

It should be stressed that the results in Fig. 9 is very sensitive to the magnitude of parameters, mainly β and \dot{M}_{peak} . The former affects the magnitude of \dot{M} as it enlarges by a factor of $1/(\beta-\beta_0)$ compared to the $\dot{\beta}$, as shown in Eq. 3. The latter, on the other hand, affects the magnitude of the disk drag, thus changing the moment of transition when β changes from increasing to decreasing.

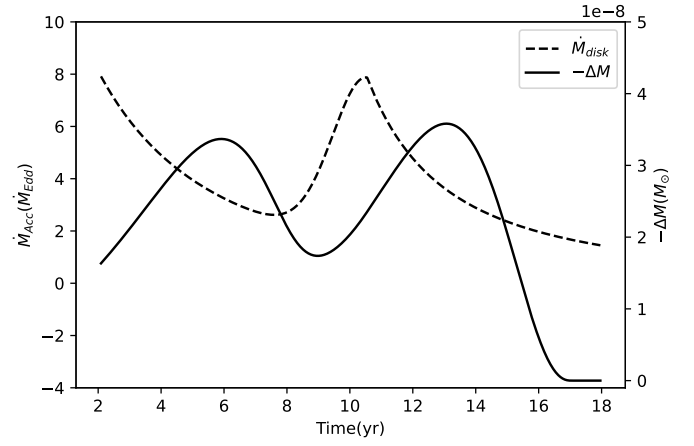


Fig. 9. Possible evolution of mass transfer with the evolution of the accretion rate of the accretion disk. Solid line and dashed line represent the evolution of the mass transfer at the periastron and the accretion rate of the disk in GSN 069, respectively. See text for details of calculations.

We do not show the evolution of the light curve directly, because the radiative processes are not considered here. If one assumes a positive correlation between the bolometric luminosity and the accretion mass, the disappearance of the QPEs in the early stages of the TDE and the lack of increase of its luminosity as well as its fading can be explained. That is, the early accreted mass increases rapidly and then starts to decrease as the disk drag increases.

However, the subsequent evolution is somewhat difficult to explain. Although the decrease in the accreted mass when the TDE flares again seems to explain the disappearance of the QPEs. But as pointed out by Miniutti et al. (2023a), the spectrum of QPEs need to be colder than it of the TDE to be undetectable, not just less luminous than the TDE. In addition, the second flare of the two QPEs that reappeared brightened, as expected in Fig. 9, yet the first flare did not brighten and could not be explained by our model.

These variations may be related to radiation processes of the QPEs. Lu & Quataert (2023) suggested that the QPEs is produced by the circularized shock of the accreted matter moving inside the disk. The peak temperature decreases during the second outburst of the TDE due to the decrease in disk density. This may explain the disappearance of QPEs. Thus the evolution of QPEs is also directly related to the evolution of accretion disk. The secular evolution on the light curve and spectrum of QPEs requires a further analysis combined with radiative processes in the future.

For the accretion model of the QPEs, the long-short behavior on the intensity and recurrence time is difficult to explain. King (2022) proposed that the short accretion timescale may cause the WD to fail to maintain hydrostatic equilibrium and oscillate in radius, which may explain this feature of QPEs. Such oscillations may be perturbed when the density of the surrounding gas changes, which may explain the disappearance of such features in QPEs before the second outburst of the TDE and the weaker QPE after this outburst that did not enhance as we expected. The evolution of such short timescales is beyond the scope of this paper, which focuses on long-term evolution.

4. Discussion

4.1. Unconservative mass transfer

It is also possible for material to be lost through the Lagrangian point L2, and this is more likely to happen for systems with high eccentricity (Sepinsky et al. 2007a). This lost material may form a circumbinary binary disk, which may significantly affect the orbital evolution (Dermine et al. 2013). I will not discuss this scenario here, but rather the case where this material leaves the binary system altogether.

Differentiating the total angular momentum gives

$$\frac{\dot{J}}{J} = \frac{\dot{M}_h}{M_h} + \frac{\dot{M}}{M} - \frac{\dot{M}_t}{2M_t} + \frac{1}{2} \frac{\dot{e}}{1+e} + \frac{1}{2} \frac{\dot{r}_p}{r_p}. \quad (25)$$

Assuming the mass transfer occurs only instantaneously at the periastron, then $\dot{r}_p = 0$. The fraction of mass that is accreted to the central black hole is defined as $\gamma = -\dot{M}_h/\dot{M}$. The mass lost by the system also carries away angular momentum. Defining that the ratio of its specific angular momentum to that of the stripped star is λ , the change of the total angular momentum is $\dot{J}/J = \lambda\dot{M}_t/qM_t$. Then Eq. (25) becomes

$$\langle \dot{e} \rangle_M = -\mathcal{F}(\gamma, q, \lambda)(1+e) \frac{\dot{M}}{M}, \quad (26)$$

where

$$\mathcal{F}(\gamma, q, \lambda) = \frac{2 + 2(\gamma - 1)\lambda + (1 - \gamma)q - 2\gamma q^2}{1 + q}. \quad (27)$$

By $\dot{r}_p = 0$, we have

$$\left\langle \frac{\dot{a}}{a} \right\rangle_M = \frac{\langle \dot{e} \rangle_M}{1 - e} = -\mathcal{F}(\gamma, q, \lambda) \frac{1 + e}{1 - e} \frac{\dot{M}}{M}. \quad (28)$$

When $\gamma = 1$, they reduce to Eq. (5) and (7).

Assuming that half the mass is lost from L2 and their specific angular momentum is the same as that of the stripped star, i.e., $\gamma = 0.5$ and $\lambda = 1$, Eq. (26) becomes

$$\langle \dot{e} \rangle_M = -\frac{1 + 0.5q - q^2}{1 + q} \frac{\dot{M}}{M}(1 + e) \approx -(1 + e) \frac{\dot{M}}{M} \left(1 - \frac{q}{2}\right). \quad (29)$$

It is about half of what it is at $\gamma = 1$, as is $\langle \dot{a}/a \rangle_M$. The change of β now is

$$\left\langle \frac{\dot{\beta}}{\beta} \right\rangle_M \approx \frac{\dot{M}}{M} \left(\zeta - \frac{1}{3} - \frac{q}{2} \right), \quad (30)$$

which is approximately same as Eq. (6) for $q \ll 1$.

In this scenario, the effect of mass transfer is about 2 times the effect of the gravitational radiation in the balance state by comparing it with the case of $\gamma = 1$ as shown in Fig. 2. So the effect of mass transfer is still dominant on the orbital evolution in the balance state for the main-sequence star.

On the other hand, in the presence of a large-scale disk, material passing through L2 is injected into the disk and then accreted by the black hole. Therefore, the loss of matter through L2 does not affect the previous results.

4.2. Extreme mass ratio inspirals

Extreme mass ratio inspirals are the potential gravitational wave sources, and they are expected to form when compact objects gradually inspiral via gravitational wave radiation after being captured in a high eccentricity orbit (Amaro-Seoane 2018). Our results show that if the mass transfer is triggered during this process, the inspiral will be terminated and thus fail to become a gravitational wave source.

4.3. On the other QPEs

GSN 069 is not the only one galaxy found to have QPEs (Giustini et al. 2020; Song et al. 2020; Arcodia et al. 2021; Chakraborty et al. 2021), but is the only one with both TDE and QPEs (Shu et al. 2018; Sheng et al. 2021; Miniutti et al. 2023b). The orbiting WD is likely captured from a binary via the Hills mechanism (Hills 1988; Wang et al. 2022), while the TDE possibly originates from a disruption of a common envelope (Wang 2023). In this situation, the fallback disk is coplanar with the orbit of the common envelope, which is almost coplanar with the orbit of the captured WD. Thus, the orbiting star moves inside the disk for GSN 069.

As for the other QPEs sources, the situation may be different. The pre-existing disk may not be present, or the pre-existing disk may be inclined to the orbit of the stripped star. In the former case, the orbital evolution is the same as discussed in Section 2. In the latter case, the effect of the disk on the orbit will be different from that discussed in Section 3. For example, Linial & Quataert (2024) found the hydrodynamic drag force received by the star as it passes through the inclined disk can make the orbital period decrease.

The TDE in GSN 069 makes it unique. On the one hand, it may be the only source whose accretion disk is coplanar with the orbit of the stripped star. On the other hand, the accretion rate of its disk is dominated by the TDE and therefore evolves rapidly. These two points lead to a complicated orbital evolution, making the QPEs in GSN 069 an excellent source to study the interaction between the disk and the object moving inside it.

5. Summary

By accounting for the effect of the mass transfer, the evolutionary path of the stripped star is different from the evolutionary only with gravitational wave radiation. The criterion of the unstable mass transfer is changed and the fate of the stripped star is to escape the SMBH rather than be disrupted by it. In this case, however, mass transfer remains unstable.

The TDE in GSN 069 may be a disruption of the common envelope before the WD was captured, so the orbiting WD is likely moving inside the fallback disk. The hydrodynamic drag force by the disk can effectively reduce β and stabilize the mass transfer, which can explain the observed long term evolution in the intensity of QPEs. After the TDE re-brightened, the mass transfer increases due to the weakening of the drag force caused by the reduced density of the inner zone of the accretion disk. As the accretion rate of the fallback disk gradually decreases, the drag force by the disk will decrease until it is negligible. Then the mass transfer will start to be unstable eventually the WD will escape the SMBH.

The spectrum evolution of QPEs is also directly related to the evolution of the accretion disk. Future work will require further quantitative analysis of the evolution of mass transfer in combination with specific radiative processes. And continued observations of GSN 096 will help us to understand the interaction of the disk with the star inside it and to test our model.

Acknowledgements. Thanks Mengye Wang for helpful discussion. This work was supported by the National Key Research and Development Program of China (No. 2020YFC2201400) and National SKA Program of China (2020SKA0120300).

References

Amaro-Seoane, P. 2018, *Living Reviews in Relativity*, 21, 4

- Arcodia, R., Merloni, A., Nandra, K., et al. 2021, *Nature*, 592, 704
- Babak, S., Gair, J., Sesana, A., et al. 2017, *Physical Review D*, 95, 103012
- Chakraborty, J., Kara, E., Masterson, M., et al. 2021, *The Astrophysical Journal Letters*, 921, L40
- Chen, J.-H., Shen, R.-F., & Liu, S.-F. 2023, *The Astrophysical Journal*, 947, 32
- Chen, X., Qiu, Y., Li, S., & Liu, F. 2022, *The Astrophysical Journal*, 930, 122
- Demircan, O. & Kahraman, G. 1991, *Astrophysics and Space Science*, 181, 313
- Dermine, T., Izzard, R., Jorissen, A., & Van Winckel, H. 2013, *Astronomy & Astrophysics*, 551, A50
- Franchini, A., Bonetti, M., Lupi, A., et al. 2023, *Astronomy & Astrophysics*, 675, A100
- Giustini, M., Miniutti, G., & Saxton, R. D. 2020, *Astronomy & Astrophysics*, 636, L2
- Hills, J. G. 1988, *Nature*, 331, 687
- King, A. 2020, *Monthly Notices of the Royal Astronomical Society: Letters*, 493, L120
- King, A. 2022, *Monthly Notices of the Royal Astronomical Society*, 515, 4344
- Krolik, J. H. & Linial, I. 2022, *The Astrophysical Journal*, 941, 24
- Linial, I. & Metzger, B. D. 2023, arXiv preprint arXiv:2303.16231
- Linial, I. & Quataert, E. 2024, *Monthly Notices of the Royal Astronomical Society*, 527, 4317
- Linial, I. & Sari, R. 2023, *The Astrophysical Journal*, 945, 86
- Lu, W. & Quataert, E. 2023, *Monthly Notices of the Royal Astronomical Society*, 524, 6247
- Luo, J., Chen, L.-S., Duan, H.-Z., et al. 2016, *Classical and Quantum Gravity*, 33, 035010
- Miniutti, G., Giustini, M., Arcodia, R., et al. 2023a, *Astronomy and Astrophysics*, 674, L1
- Miniutti, G., Giustini, M., Arcodia, R., et al. 2023b, *Astronomy and Astrophysics*, 670, A93
- Miniutti, G., Saxton, R., Giustini, M., et al. 2019, *Nature*, 573, 381
- Ostriker, E. C. 1999, *The Astrophysical Journal*, 513, 252
- Paczynski, B. 1971, *Annual Review of Astronomy and Astrophysics*, 9, 183
- Peters, P. C. 1964, *Physical Review*, 136, B1224
- Sepinsky, J., Willems, B., & Kalogera, V. 2007a, *The Astrophysical Journal*, 660, 1624
- Sepinsky, J., Willems, B., Kalogera, V., & Rasio, F. 2007b, *The Astrophysical Journal*, 667, 1170
- Shen, R.-F. & Matzner, C. D. 2014, *The Astrophysical Journal*, 784, 87
- Sheng, Z., Wang, T., Ferland, G., et al. 2021, *The Astrophysical Journal Letters*, 920, L25
- Shu, X., Wang, S., Dou, L., et al. 2018, *The Astrophysical Journal Letters*, 857, L16
- Song, J., Shu, X., Sun, L., et al. 2020, *Astronomy & Astrophysics*, 644, L9
- Suková, P., Zajaček, M., Witzany, V., & Karas, V. 2021, *The Astrophysical Journal*, 917, 43
- Szölgény, Á., MacLeod, M., & Loeb, A. 2022, *Monthly Notices of the Royal Astronomical Society*, 513, 5465
- Wang, D. 2023, arXiv preprint arXiv:2312.01737
- Wang, M., Yin, J., Ma, Y., & Wu, Q. 2022, *The Astrophysical Journal*, 933, 225
- Xian, J., Zhang, F., Dou, L., He, J., & Shu, X. 2021, *The Astrophysical Journal Letters*, 921, L32
- Zalamea, I., Menou, K., & Beloborodov, A. M. 2010, *Monthly Notices of the Royal Astronomical Society: Letters*, 409, L25
- Zhao, Z., Wang, Y., Zou, Y., Wang, F., & Dai, Z. 2022, *Astronomy & Astrophysics*, 661, A55